Stress Relaxation and Reconstruction of the Associating Network in Semidilute Aqueous Solutions of Hydrophobically Modified Random Block Copolymers

R. Klucker[†] and F. Schosseler*

Laboratoire de Dynamique des Fluides Complexes, Université Louis Pasteur, 4 rue Blaise Pascal, 67070 Strasbourg Cedex, France

Received February 4, 1997; Revised Manuscript Received June 3, 1997[⊗]

ABSTRACT: We study the transient rheological behavior of associating polyacrylamide-based copolymers in aqueous solution. We measure the characteristic times associated with the stress relaxation after a shear step and with the reconstruction of the transient associating network after its destruction by the shear. These characteristic times differ by 2−4 orders of magnitude depending on the applied shear rate. The stress relaxation is rapidly dominated by the free chains and the small clusters arising from the destruction of the associating network. The latter is related to a large-scale texture that needs very long times (up to 4×10^4 s) to re-form after its destruction by the shear.

Introduction

Associating polymers in solution display a variety of rheological behaviors depending on their achitecture and their concentration.[1−3] Usually the zero-shear viscosity increases rapidly with polymer concentration and is considerably larger than those in solutions of nonassociating polymers with comparable molecular weight and concentration. This effect results from the formation of a transient associative network, with intermolecular associations being favored by the increase of polymer concentration, at the expense of the intrachain associations that are observed in dilute solutions.

Upon an increase of the shear rate, an extended Newtonian behavior followed by shear-thinning effects is usually observed for the steady-state viscosity in solutions of short chains with associative end groups. However, the shear flow can also increase the probability of forming interchain associations by extending the conformation of the chains,[4] and some instances of shear-thickening behavior have been reported at intermediate values of the shear rate for solutions of end-modified short chains[4−6] as well as for solutions of randomly modified long chains in an entangled regime.[7,8]

Recently, interesting hysteresis effects have been reported[9] for the steady-state viscosity vs shear rate behavior of aqueous semidilute solutions of long polyacrylamide chains with randomly distributed blocks of hydrophobic units: the steady-state viscosity values measured in a thixotropic loop, where the shear rate is first increased and then decreased back to its initial value, were found to be significantly smaller in the down sequence than in the up sequence. Only after several hours of rest was the initial zero-shear viscosity of the samples recovered. Although this phenomenon can evidently be related to the destruction of the transient associative network upon shearing and to its very slow reconstruction afterward, it is not clear which are the mechanisms involved.

In particular, an intuitive picture of the system would depict it as a semidilute solution with some hydrophobic associations into domains acting as temporary cross-links that enhance both the plateau modulus and the longest relaxation time in the solution, thus leading to an increase of the shear viscosity. However, in that simple picture, the reconstruction of the associative network involves essentially local mechanisms, linked to the reorganization and the reassociation of the disrupted domains with a time scale mainly given by the cooperative dynamics of the chains. Then their reptation time is the longest characteristic time in the system,[10] and even if sticky reptation,[11] i.e., reptation slowed down by the temporary associations, is taken into account, the characteristic time scales involved in the reconstruction of the associating network could be expected to remain comparable to those involved in the stress relaxation.

However, previous experiments have shown qualitatively that the stress relaxation is apparently much faster than the recovery of the initial properties of the solution and that its time scale depends on the applied shear rate.[12] The present paper is aimed at providing a more quantitative description of these effects and comparing the time scales involved in the stress relaxation and in the reconstruction of the associative network after its destruction.

Experimental Section

1. Sample Synthesis and Characterization. The samples are synthesized by the micellar radical copolymerization, in presence of sodium dodecyl sulfate (SDS) surfactant, acrylamide, and *N*-(4-ethylphenyl)acrylamide monomers. The principles of and conditions of the synthesis have been fully described elsewhere.[8,13,14] The presence of the surfactant (3% w/w based on the total amount of water solvent) allows the solubilization of the hydrophobic monomer (molar feed fraction 0.0075, based on the total amount of monomers). The reaction is initiated by potassium persulfate. The blockiness of the copolymers results from the polymerization proceeding alternately in the aqueous bulk solution and inside the micelles. However, due to effects discussed at length in previous papers,[8,9,13,14] a drift in the average copolymer composition is observed for samples obtained at full conversion. This drift can be avoided by stopping the reaction before completion through the addition of hydroquinone. The polymers are then precipitated in methanol and washed repeatedly with methanol to remove unreacted species and surfactant. After careful drying the polymers are stored in air-tight containers before use. The weight-average molecular weight of the samples is measured by static light scattering in dilute formamide

[†] Present address: Centre de Recherches Paul Pascal, Avenue Schweitzer, 33600 Pessac, France.

[⊗] Abstract published in *Advance ACS Abstracts,* July 15, 1997.

S0024-9297(97)00158-7 CCC: $14.00

Table 1. Characteristics of the Samples

	polymerization parameter		polymer characterization		
sample	[SDS][a]	hydrophobe conc.[b]	conversion (%)	hydrophobe content (mol %)	M_w ($\times 10^6$)
I	3	0.75	9.2	1.10	3.0
J	3	0.75	13	1.14	4.0

[a] SDS weight percent in the feed, based on volume of water. [b] Mole percent in the feed, based on monomer concentrations. [c] Weight percent based on initial monomer amount.

solutions, and their hydrophobe content is obtained through UV spectroscopy measurements. Table 1 summarizes the characteristics of the samples used in this study.

2. Rheological Measurements. The rheological experiments are performed with a Rheometrics RFS II fluid rheometer equipped with a cone−plate tool (radius 2.5 cm, angle 0.0397 rad, gap 45 μm) and a homemade device that prevents evaporation of the samples during experiments with long duration times. This device consists of two flat cylindrical pieces pierced with a hole in their center. The upper one is fitted to the shaft of the transducer, while the bottom one is fixed to the frame of the rheometer, surrounding without contact the shaft of the motor. The bottom piece has a U-shaped edge that is filled with water or oil. The two pieces are brought together so that the edge of the top one is below the level of the liquid contained in the edge of the bottom one. In this way a freely-rotating air-tight cavity around the tool can be formed. The torque generated by the friction between the top edge and the liquid and also the buyoancy force are negligible. The weight of the top piece introduces in the value measured by the normal force transducer a constant off-set that has to be taken into account.

Samples for the rheological measurements are prepared by adding to a given amount of polymer the appropriate quantity of deionized water to obtain a 3% w/w concentration. The chains are allowed to hydrate and swell for 24 h. Then the sample is very gently stirred for another 24 h duration. After 2 days more, the sample is ready for measurements. It is gently loaded into the cone−plate tool and given a rest of half an hour before the beginning of the measurements. Different rest times have been tried, and it appears that, with these samples, half an hour is long enough to allow reproducible results that are identical within experimental errors to the ones obtained after larger rest times about 3 h.

In the experiments we apply successive shear rate steps with amplitude $\dot{\gamma}$ and duration Δt, separated by a rest time T. Interesting information is contained in the steady-state value of the stress measured for long enough time t but also in the rise of the stress at the beginning of the shear step, as shown in a previous paper,[12] and in the stress relaxation after the cessation of the shear.

However, the investigation of transient rheological behavior is made more difficult by the presence of inertial effects that limit the ability of the apparatus to generate ideal rectangular shear rate steps. Thus, at the startup of the steps, a finite time is needed to accelerate the plate until the steady-state angular velocity is reached and there is a difference between the actual accumulated strain and the expected one. This difference can be easily characterized and taken into account by performing experiments with Newtonian oils and establishing a correspondence between elapsed time and accumulated deformation, as described in a previous paper.[12]

On the other hand, at the cessation of the shear, inertial effects result in dumped oscillations of the plate that can be easily observed with a Newtonian oil as shown in Figure 1. The amplitude of these oscillations is independent of the applied shear rate and appears relatively more important for the smallest shear rates when the stress normalized by its value at the cessation of the shear is plotted as in Figure 1. These oscillations should have only a small effect on the stress relaxation of the samples since the associated strain variations are small, but they prevent the characterization of relaxation times shorter than about 0.3 s. Usually this is not too much of a problem since the stress relaxation times in our associating polymer solutions are often much longer and can be as high as a few hundreds of seconds. In fact, these long relaxation times can even introduce artifacts if the rest time between two successive steps is not large compared to the stress relaxation times, since the apparatus performs before each step an automatic calibration procedure that sets the initial recorded stress as the zero. This has to be taken into account when experiments using successive steps are done.[12]

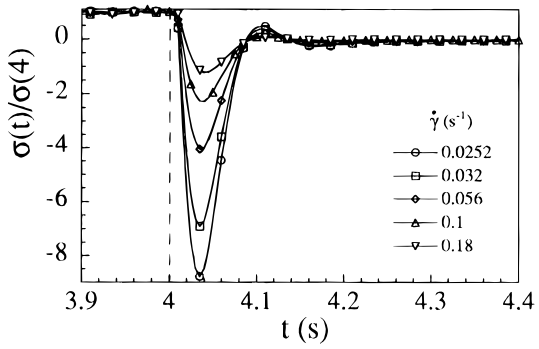

Figure 1. Normalized stress measured after the cessation of a shear step for a Newtonian silicone oil. An ideal step should stop at $t = 4$ s (vertical dashed line). One data point out of five is marked by a symbol.

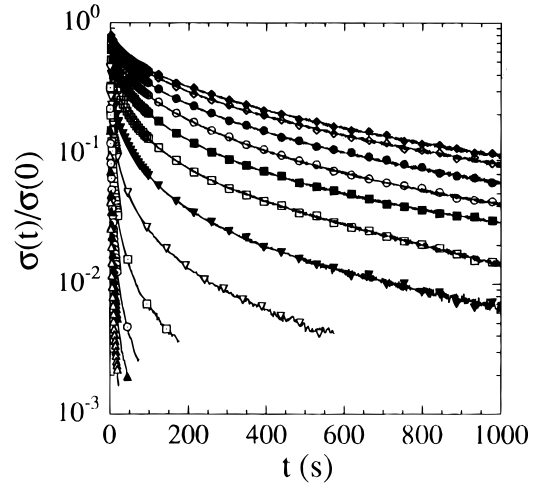

Figure 2. Normalized stress measured after the cessation of a shear step with varying shear rate (copolymer I, $C = 3\%$ w/w). Values of the shear rate $\dot{\gamma}$ (s^{-1}) are, from top to bottom, 0.0252, 0.032, 0.056, 0.1, 0.18, 0.32, 0.56, 1, 1.8, 3.2, 5.6, and 10. One data point out of 20 is marked by a symbol.

Results

1. Stress Relaxation. Figure 2 shows the evolution with shear rate amplitude of the normalized stress relaxation curves for a copolymer solution with a 3% w/w concentration. As the shear rate $\dot{\gamma}$ increases, the relaxation becomes faster. A closer examination of the curves allows one to distinguish two features that are responsible for that effect. First, as the shear rate increases, a larger part of the relaxation takes place on a short time scale, while the longest relaxation times appear essentially unaltered. For shear rates above 0.32 s^{-1}, on the other hand, an additional effect appears that is the long-time decay becoming faster and faster with increasing shear rate.

It can be noted that only stress values corresponding to torque values above the sensitivity limit of the transducer are plotted in Figure 2. In ref 12, values below this limit were incorrectly kept, thus leading to a nonzero plateau behavior at long time in the representation of Figure 2.

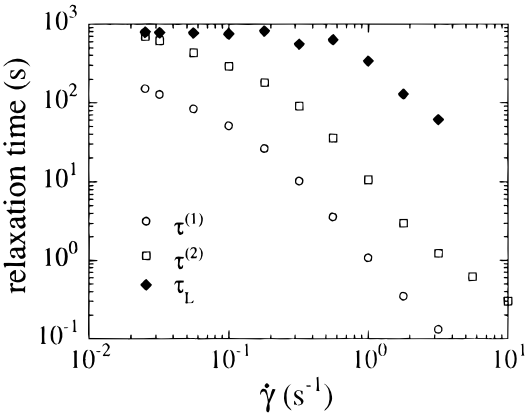

Figure 3. Variation with applied shear rate of the relaxation times defined in the text for the stress relaxation curves in Figure 2.

The features in Figure 2 are consistent with the idea that the transient associative network is increasingly disrupted by the shear flow as $\dot{\gamma}$ is increased. Thus, a growing part of the stress relaxation can occur through the motion of nonassociated chains that move with rather fast dynamics compared to the associated chains. This picture can be given a more quantitative meaning by defining some characteristic times: the longest relaxation time τ_L can be obtained by fitting the long-time behavior as single-exponential and average decay times $\tau^{(1)}$, $\tau^{(2)}$, respectively, and can be defined as the times where the normalized stress has decayed by a factor $1/e$ and $1/e^2$, respectively. The experimental values of τ_L, $\tau^{(1)}$, and $\tau^{(2)}$ corresponding to the stress relaxation curves in Figure 2 are plotted in Figure 3 as a function of the applied shear rate.

It appears clearly that the longest relaxation time τ_L keeps a constant value of about 800 s for shear rates below 0.2 s^{-1} and starts to decrease for larger $\dot{\gamma}$ values. On the other hand, the average times $\tau^{(1)}$ and $\tau^{(2)}$ decrease continuously as $\dot{\gamma}$ increases, and the ratios between τ_L and these average values increase by about 2 orders of magnitude over the $\dot{\gamma}$ range investigated here. The evolution of these ratios reflects the growing contribution of fast relaxation processes as the shear flow breaks the associations.

A different analysis of the curves in Figure 2 can be done by fitting them as a sum of exponential functions, i.e.

$$\sigma(t)/\sigma(0) = \sum_{i=1}^{N} p(\tau_i) \exp(-t/\tau_i) \qquad (1)$$

where $p(\tau_i)$ and τ_i are positive parameters. This fitting procedure is easily performed with the program CONTIN,[15] which is widely used for the analysis of data obtained by photon correlation spectroscopy.[16] The rheological data can be processed by the same means as well after suitable data file shaping. For the curves in Figure 2, the time window used in the fitting procedure was chosen to lie in the range $5 \times 10^{-2} \leq \tau_i$ (s) $\leq 10^4$ and the number of time bins N in eq 1 was set to 40. The CONTIN procedure divides the time window into N intervals with equal width on a logarithmic scale.

A practical problem arises because of the limitation on the maximum number of data points (256) allowed for an analysis in a reasonable time (a few tens of seconds). Thus, it is necessary to reduce the number of experimental points (usually about 1600) in each

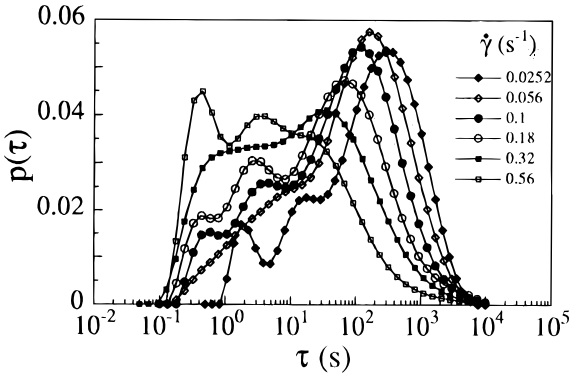

Figure 4. CONTIN analysis of the stress relaxation curves in Figure 2.

curve of Figure 2. This is done by interpolation through the experimental curves for t values spaced regularly on a logarithmic scale and spanning the whole experimental range. This particular spacing of the interpolated points is chosen because it is more consistent with the way CONTIN is running and it avoids overweighing some regions in the relaxation curves due to the linear spacing of measurement times in the rheometer acquisition software. However, we checked that the main features of the resulting $p(\tau)$ functions do not depend on the spacing of the analyzed data points. These functions are shown in Figure 4.

As the shear rate is increasing, there is a progressive shift to shorter times of the maximum of $p(\tau)$. It can be noted that the growing contribution of the fast relaxation processes is not clearly apparent in Figure 4 due to the spoiling of the results by the inertial effects described in the Experimental Section. Due to these effects, the part of the amplitude $p(\tau)$ for τ smaller than about 0.5 s is not reliable. The most interesting information brought by the CONTIN analysis in this case is the continuous evolution of the shape of the $p(\tau)$ curve in the large τ region, even for the lowest shear rates investigated here. Although the longest relaxation time $\tau_L \sim 800$ s remains constant at low shear rates (Figure 3), $p(\tau \approx \tau_L)$ is decreasing continuously (Figure 4). This indicates that the shear flow is already affecting the transient associative network even for very small values of the shear rate.

Thus, although the experimental results in Figures 2 and 3 might suggest that the stress relaxation is governed by two distinct time scales, the evolution of the amplitude $p(\tau)$ is, in fact, continuous, and Figure 4 shows no threshold value of the shear rate above which the destruction of the associative network would begin. It is more likely that, for any shear rate value, there is a stationary distribution of associated clusters which displays all sizes of clusters from the free chain to a characteristic size depending on the shear rate. This situation might reflect the experimental procedure used here since the duration $\Delta t = 1000$ s of each shear step was long enough to reach the steady-state value of the stress.

It should be emphasized here that the amplitudes $p(\tau)$ are not linked in a simple way to the distribution of connected cluster sizes that characterizes the disrupted transient associative network. In fact, the fastest relaxation processes can dominate the stress relaxation even if very large connected clusters still exist. This was recognized a long time ago for systems of polymer stars immersed in a melt of linear chains.[10,17]

2. Influence of Shear History on Stress Relaxation. So far we have studied the stress relaxation

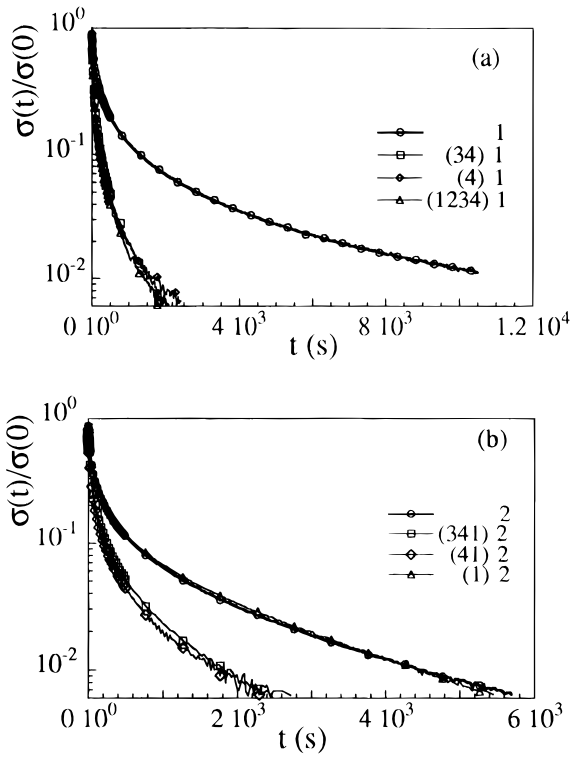

Figure 5. Influence of shear history on the stress relaxation measured after a shear rate step with amplitude $\dot{\gamma} = 0.05$ s^{-1} (a) and $\dot{\gamma} = 1$ s^{-1} (b). The numbers in parentheses indicate the shear steps performed before the actual measurement (see text). One data point out of 20 is marked by a symbol. The sample is copolymer J with $C = 3\%$ w/w.

during successive shear rate steps with increasing amplitude, and we have implicitly assumed that, in these conditions, the stress relaxation for a given shear rate step is not influenced by the preceding steps. This has to be checked since the rise of the stress was previously found to be highly dependent on the shear history.[12] Therefore, we designed an experiment where successive shear rate steps with four different magnitudes were applied in varying order. The amplitudes are $\dot{\gamma}_1 = 0.05$ s^{-1}, $\dot{\gamma}_2 = 0.1$ s^{-1}, $\dot{\gamma}_3 = 1$ s^{-1}, and $\dot{\gamma}_4 = 10$ s^{-1}. The duration $\Delta t = 3600$ s of each step and the rest time $T = 10\,800$ s between them are kept constant. Figure 5 shows some typical relaxation curves measured after a shear rate step with amplitude $\dot{\gamma}_1$ (Figure 5a) or $\dot{\gamma}_2$ (Figure 5b) with different preceding shear histories, indicated in the brackets by the indices of the successive applied shear rates.

The behavior of the relaxation curves in Figure 5 shows clearly that the stress relaxation after a step with a given shear rate value $\dot{\gamma}_i$ is not affected by the preceding shear history as long as the latter does not contain steps with shear rates larger than $\dot{\gamma}_i$. In the latter case, the shape of the relaxation curve is given by the step with the highest shear rate. These observations validate the results presented above. Moreover, they are consistent with (i) the achievement of a steady-state breaking of the associating network through shear steps with long enough duration and (ii) a reconstruction time much larger than the characteristic times involved in the relaxation of the stress.

3. Structural Recovery of the Associating Network after Shearing. The preceding results suggest a method to study the recovery of the initial properties of the solutions after a shear flow has broken the

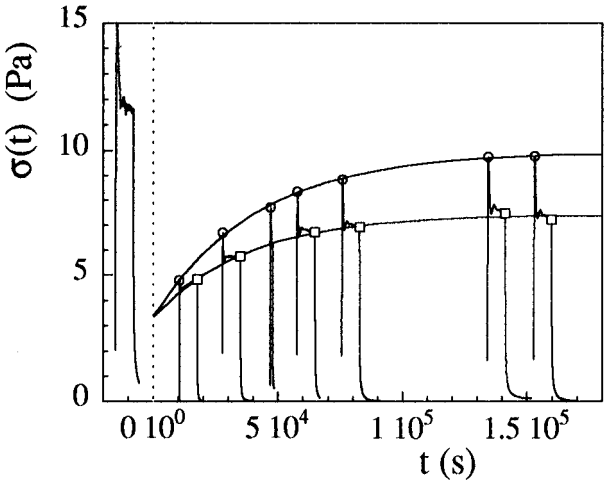

Figure 6. Evolution of the shear stress during successive shear steps with $\dot{\gamma}_t = 0.05$ s^{-1} as a function of time elapsed since a shear step (not shown in the Figure) with a large amplitude $\dot{\gamma}_p = 10$ s^{-1} has been applied. Time origin corresponds to the end of the latter shear step (dotted line). For the sake of comparison, the stress recorded during a shear step with $\dot{\gamma}_t = 0.05$ s^{-1} performed prior to the perturbation is shown (arbitrary negative values of the time). The circles and squares correspond to the overshoot stress values σ_{max} and the stress values σ_{7200} measured after 7200 s, respectively. The continuous lines through these points show the fits obtained with eq 2 in the text (copolymer J, $C = 3\%$ w/w).

associating network. On a fresh sample, we apply first a shear rate step with small amplitude $\dot{\gamma}_t = 0.05$ s^{-1} ($\Delta t = 7200$ s) that allows one to measure the initial stress curve of the sample. Then the system is strongly perturbated by a shear step with $\dot{\gamma}_p = 10$ s^{-1} ($\Delta t = 7200$ s). The reconstruction of the system can then be tested by using shear steps with amplitude $\dot{\gamma}_t$ and varying the elapsed time since the cessation of the perturbation. Figure 6 shows the evolution, as a function of elapsed time, of the stress recorded during the succession of steps.

It appears readily that the shape of the stress curves depends on the elapsed time. In particular, the amplitude of the stress overshoot relative to the value of the stress after 7200 s (duration of the step) increases with elapsed time, as reported previously.[12] It can also be noticed that, at the end of each step, there is no indication for the achievement of a steady-state stress value. This fact is indeed due to the continuous reconstruction of the sample during the experiment as we checked that, during the initial step with $\dot{\gamma}_t = 0.05$ s^{-1}, a duration $\Delta t = 7200$ s was long enough to ensure a stationary value for the stress.

Figure 7 shows the evolution of the normalized stress relaxation curves measured at the end of each step in Figure 6. The initial curve displays very long characteristic times, while the first stress relaxation measured after the perturbation is reminiscent of the behavior in Figure 5. As the elapsed time increases, longer relaxation times appear again and the stress relaxation curves become closer and closer to the initial curve.

The reconstruction of the associative network can be analyzed more quantitatively by looking at the time evolution of the values for the stress overshoot $\sigma_{max}(t)$ and for the stress $\sigma_{7200}(t)$ measured after 7200 s of applied shear. As shown in Figure 6, the evolution of $\sigma_{max}(t)$ (shown by circles) and of $\sigma_{7200}(t)$ (shown by squares) can be fitted quite satisfactorily with a single-exponential relaxation as

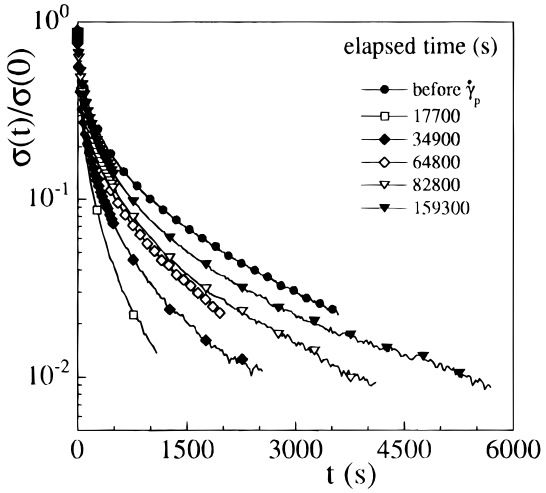

Figure 7. Evolution of the normalized stress relaxation curves measured after the shear steps in Figure 6. One data point out of 20 is marked by a symbol.

$$f(t) = f^{(0)}(\dot{\gamma}_p,\dot{\gamma}_t) + [f^{(\infty)}(\dot{\gamma}_p,\dot{\gamma}_t) - f^{(0)}(\dot{\gamma}_p,\dot{\gamma}_t)][1 - \exp(-t/\tau_r)] \quad (2)$$

where $f(t)$ is either $\sigma_{max}(t)$ or $\sigma_{7200}(t)$ and the meaning of the quantities $f^{(0)}(\dot{\gamma}_p,\dot{\gamma}_t)$, $f^{(\infty)}(\dot{\gamma}_p,\dot{\gamma}_t)$, and τ_r is given below.

After perturbation by the step with amplitude $\dot{\gamma}_p$, we obtain a steady-state rupture of the associated network related to $\dot{\gamma}_p$. Thus $f^{(0)}(\dot{\gamma}_p,\dot{\gamma}_t)$ would be the value of $f(t)$ if we were able to measure its stationary value with a shear rate $\dot{\gamma}_t$ and without any structural recovery taking place. In particular, the limit for vanishing $\dot{\gamma}_t$ of $\sigma^{(0)}_{7200}(\dot{\gamma}_p,\dot{\gamma}_t)/\dot{\gamma}_t$ is the zero-shear viscosity of the perturbated associating solution. Interestingly, $\sigma^{(0)}_{max}(\dot{\gamma}_p,\dot{\gamma}_t)$ and $\sigma^{(0)}_{7200}(\dot{\gamma}_p,\dot{\gamma}_t)$ are found to be identical within experimental errors (see Figure 6). This means that no stress overshoot would be observed in a hypothetical experiment with no reconstruction taking place, and this is consistent indeed with the previously reported influence of shear history on stress overshoots in these systems.[12]

In an obvious way, $f^{(\infty)}(\dot{\gamma}_p,\dot{\gamma}_t)$ in eq 2 is the value for $f(t)$ at infinite reconstruction time, and thus it is a quantity that should, in principle, not depend on the applied perturbation before time origin if final thermodynamic equilibrium is assumed. On the other hand, if the system can be quenched in metastable states, then the final state may depend on the route followed beforehand.

Finally τ_r in eq 2 is a characteristic time for the recovery of the quantity $f(t)$ due to the reconstruction of the associating network between the two steady states corresponding respectively to shear rates $\dot{\gamma}_p$ and $\dot{\gamma}_t$. The same remarks as for $f^{(\infty)}(\dot{\gamma}_p,\dot{\gamma}_t)$ apply concerning its dependence as a function of $\dot{\gamma}_p$ and $\dot{\gamma}_t$.

Surprisingly, only one relaxation time is needed to describe the time evolution of $\sigma_{max}(t)$ and $\sigma_{7200}(t)$. In both cases, we get the same value for τ_r within experimental errors, i.e. $\tau_r = 41\,800 \pm 2400$ s (σ_{max}) and $\tau_r = 38\,100 \pm 5700$ s (σ_{7200}). We note for further comparison the values $\sigma^{(0)}_{7200} = 3.51 \pm 0.18$ Pa and $\sigma^{(\infty)}_{7200} = 7.63 \pm 0.32$ Pa.

A similar analysis with the help of eq 2 can be performed for the evolution of the average times $\tau^{(1)}$ and $\tau^{(2)}$ estimated from the data in Figure 7. Here again a single relaxation time is sufficient to describe the time evolution of $\tau^{(1)}$ and $\tau^{(2)}$ due to the reconstruction of the transient associative network. In this case also we get comparable values within experimental errors, $\tau^{(1)}_r = 77\,000 \pm 30\,000$ s ($\tau^{(1)}$) and $\tau^{(2)}_r = 90\,000 \pm 45\,000$ s ($\tau^{(2)}$). Although the very large error bars do not strictly allow to one distinguish these values from the ones determined from the evolution of the stresses, there is, however, no reason to expect the same recovery time value for the stresses and for the average times defined above since these quantities correspond to different combinations of the moduli and relaxation times in the relaxation spectrum.

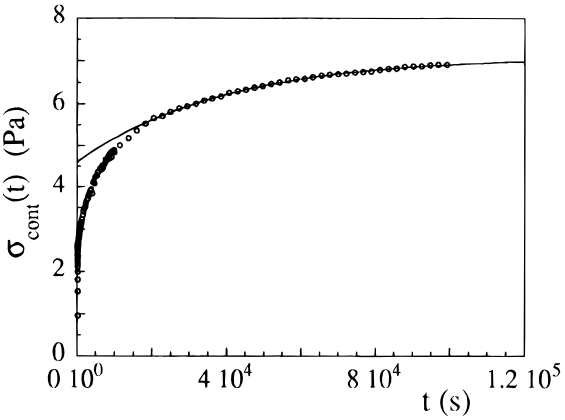

Figure 8. Evolution of the stress measured during a shear step with $\dot{\gamma}_t = 0.05$ s^{-1} performed immediately after the cessation of a shear step with $\dot{\gamma}_p = 10$ s^{-1} (copolymer J, C = 3% w/w). One data point out of 10 is marked by a symbol. The continuous line is the fit of eq 2 to the experimental values for $t \geq 21\,000$ s.

4. Effect of a Steady Shear Flow on the Structural Recovery. The reconstruction of the associating network after a strong perturbation ($\dot{\gamma}_p = 10$ s^{-1}) can also be followed by continuously measuring the evolution of the shear stress in the sample submitted to a steady shear rate $\dot{\gamma}_t = 0.05$ s^{-1}. The resulting $\sigma_{cont}(t)$, shown in Figure 8, displays a steady rise without overshoot to reach finally a plateau value after very long times larger than 10^5 s. The final part of this rise, for $t \geq 21\,000$ s, can again be described by eq 2, yielding $\tau_r = 38\,300 \pm 250$ s, $\sigma^{(0)}_{cont} = 4.59 \pm 0.01$ Pa, and $\sigma^{(\infty)}_{cont} = 7.09 \pm 0.03$ Pa.

These values compare fairly well with those obtained above, through the intermittent testing of the sample, from the evolution of the stress measured after 7200 s. Comparison shows that the final value of the stress and the characteristic times for the reconstruction of the associating network do not depend on the testing procedure. This seems to suggest that they are equilibrium values that do not depend on the applied perturbation $\dot{\gamma}_p$. However, we note that the final values $\sigma^{(\infty)}_{7200}$ and $\sigma^{(\infty)}_{cont}$ are well below the value $\sigma_{7200} = 11.6$ Pa measured prior to the shear step with $\dot{\gamma}_p = 10$ s^{-1} (Figure 6). Such an incomplete recovery of the initial properties was already observed[12] for the characteristics of the stress overshoots and was tentatively attributed to a possible aging of the sample in the tool. The reproducibility of this effect suggests that the shear might affect the sample in an irreversible way. The breaking of the chains does not appear very likely for the low shear rates (≤ 10 s^{-1}) investigated here, but it should be kept in mind that the stress can reach fairly high values due to the large viscosity of the samples. Another possibility is that the samples are never in an

equilibrium state and that we always observe metastable states that are highly dependent on the preparation and shear histories. This point would deserve more experiments to be fully clarified, and, in particular, degradation of the samples under shear should definitely be ruled out by molecular weight characterization prior to and after the shear steps.

It can also be noted that the early stage of the reconstruction seems to be faster in the case of a continuous shearing of the sample, resulting in a value of $\sigma_{cont}^{(0)}$ somewhat larger than the corresponding $\sigma_{7200}^{(0)}$ value. Here again more experiments would be needed to confirm that point. If true, it could be explained by an increased probability for hydrophobic blocks belonging to different clusters to recombine due to the alignment and extensions of the connected regions in the shear flow. A similar mechanism has been proposed[4,7] to explain the shear thickening behavior of some associating polymer solutions. In the case of our samples, however, this type of behavior was not observed. It can be remarked that the small value of $\dot{\gamma}_t$ used here seems to rule out an influence of the shear flow on the conformation of free chains or small clusters.

Discussion and Conclusion

The results presented above show that the stress relaxation and the recovery of the initial properties have very different time scales. After a shear step with amplitude $\dot{\gamma}_p = 10\ s^{-1}$, most of the stress relaxes on time scales smaller than 1 s (Figure 7), while it is necessary to wait for about 4×10^4 s to reach the stationary state of the reconstructing solution as measured by a shear step with small amplitude $\dot{\gamma}_t = 0.05\ s^{-1}$. This fast stress relaxation is due to the achievement of a steady-state breaking of the hydrophobic associations by the shear flow and to a dominant contribution of free chains and small clusters in the relaxation process. In fact, a previous estimation[12] of the disengagement time of polyacrylamide chains with $M_w \approx 1.7 \times 10^6$ at the same concentration gave a value about 1 s, consistent with the behavior observed here for chains with $M_w \approx 4 \times 10^6$.

A likely explanation for the very different orders of magnitude of the relaxation and recovery time scales could be the small concentration of hydrophobic blocks, implying that a large number of configurations must be explored before a successful meeting of hydrophobic blocks occurs. Unfortunately, due to intermicellar exchange of the hydrophobic monomers during the polymerization,[9,13,14] we are unable to calculate meaningful estimations for the mean number and the average length of the hydrophobic blocks distributed along the chains. Nevertheless, taking the simplest assumption that the block length is given by the mean number of hydrophobic units per micelle (≈1.9) and using the composition measured by UV spectroscopy (Table 1), we obtain a minimal boundary value of about 200 for the average number of acrylamide units between two blocks and a maximal boundary value of about 200 for the average number of blocks in a chain. Thus, binary contacts between hydrophobic blocks should be rather rare events.

An additional factor comes into play that is the slowing down of the dynamics of fluctuations of concentration as the association takes place. Recently, we performed detailed radiation scattering experiments[18,19] to probe the structure and the dynamics of these associating solutions on length scales between 10 and 2000 Å and on time scales between 10 ms and 50 s. We found that their structure is characterized by two distinct length scales. The first one is given by the usual correlation length ξ of a semidilute solution[20] and is about 50−100 Å for a polymer concentration of about 0.03 g/cm^3. In contrast with the picture of an ideal semidilute solution that would be homogeneous on length scales larger than ξ,[20] we also found evidence for large fluctuations of polymer concentration with a characteristic length larger than 2000 Å and with relaxation times in the range 1 ms to 10 s.

These large-scale fluctuations were given the name of "texture" because they correspond to a departure from the structure of an ideal semidilute solution, i.e., to a structure of defects. Interestingly, we found that, on the length scales probed by the dynamic light scattering technique, the characteristic relaxation time τ of the texture corresponds to internal mode dynamics and is given by

$$\tau^{-1}(q) = \frac{k_B T}{6\pi\eta} q^3 \qquad (3)$$

where q is the scattering wavevector ($5 \times 10^{-4} < q$ (Å^{-1}) $< 3 \times 10^{-3}$), $k_B T$ the thermal energy, and η a viscosity. Experimentally η was found to be close to the zero-shear viscosity of an equivalent polymer solution without hydrophobic associations, thus suggesting a viscoelastic coupling of the texture to the surrounding solution.[19] Moreover, it was shown that the main difference in the structure of polyacrylamide and hydrophobically modified polyacrylamide solutions is related to their different textures on large length scales. Thus, it is tempting to link the viscosifying properties of the associating solutions to an effect of the texture.

A somewhat similar picture of these associating solutions was inferred from their transient shear flow behavior. The features associated with the multiple overshoots observed in the stress vs time curves upon applying shear rate steps led to the conclusion that the transient associative network is loosely connected and that free chains are always present in the solution.[12]

Following these ideas, the hysteresis effects observed in the steady-state shear viscosity vs shear rate behavior should then be linked to the destruction of the texture by the shear flow and to the long time needed to reconstruct it. This long time results from the large length scales involved, from the low probability of binary contacts between hydrophobic blocks, and from the slowing down of the dynamics by the viscoelastic coupling to the surrounding solution. Moreover, it seems that the initial properties are never fully recovered and that the final state of the sample is different from its initial state.

As a concluding remark, it can be noted that the fast relaxation of the stress in our experiments is linked to our particular choice for the shear history, i.e., to the choice of long enough shear rate step that ensures a steady-state rupture of the associating structure. While this shear history is well suited for the purpose of practical applications, interesting information could be obtained as well by measuring the relaxation modulus after a step strain in the linear and nonlinear regime. Finally, the physical picture proposed here could be checked by static and dynamic light scattering experiments performed after shear steps. These experiments are currently under way.

Acknowledgment. This work was initiated by S. J. Candau, and we thank him for his continuous support

and interest. We are grateful to J. P. Munch for many stimulating discussions that have continuously influenced this work during its progress. The synthesis of the samples has been performed in the laboratory of F. Candau and J. Selb, and we gratefully acknowledge their valuable advices and many discussions about the chemical microstructure of the samples. This work has been supported by a PIRMAT joint program.

References and Notes

(1) *Polymers in Aqueous Media: Performance through Association*; Glass, J. E., Ed.; Advances in Chemistry Series 223; American Chemical Society: Washington, DC, 1989.
(2) McCormick, C. L.; Bock, J.; Schulz, D. N. In *Encyclopedia of Polymer Science and Engineering*, 2nd ed.; Wiley-Interscience: New York, 1989; Vol. 17, p 730.
(3) *Hydrophilic Polymers: Performance with Environmental Acceptability*; Glass, J. E., Ed.; Advances in Chemistry Series 248; American Chemical Society: Washington, DC, 1996.
(4) Witten, T. A.; Cohen, M. H. *Macromolecules* **1985**, *18*, 1915.
(5) Annable, T.; Buscall, R.; Ettelaie, R.; Whittlestone, D. *J. Rheol.* **1993**, *37*, 695.
(6) François, J.; Maitre, S.; Rawiso, M.; Sarazin, D.; Beinert, G.; Isel, F. *Colloid Surf.* **1996**, *A113*, 253.
(7) Ballard, M. J.; Buscall, R.; Waite, F. A. *Polymer* **1988**, *29*, 1287.
(8) Volpert E.; Selb, J.; Candau, F. *Macromolecules* **1996**, *29*, 1452.
(9) Hill, A.; Candau, F.; Selb, J. *Macromolecules* **1993**, *26*, 4521.
(10) Doi, M.; Edwards, S. F. *The Theory of Polymer Dynamics*; Oxford University Press: Oxford, U.K., 1987.
(11) Leibler, L.; Rubinstein, M.; Colby, R. H. *Macromolecules* **1991**, *24*, 4701.
(12) Klucker, R.; Candau, F.; Schosseler, F. *Macromolecules* **1995**, *28*, 6416.
(13) Hill, A.; Candau, F.; Selb, J. *Prog. Colloid Polym. Sci.* **1991**, *84*, 61.
(14) Biggs, S.; Hill, A.; Selb, J.; Candau, F. *J. Phys. Chem.* **1992**, *96*, 1505.
(15) Provencher, S. W. *Comput. Phys. Commun.* **1982**, *27*, 213.
(16) *Dynamic Light Scattering: the Method and Some Applications*; Brown, W., Ed.; Monographs on the Physics and Chemistry of Materials 49; Oxford University Press: Oxford, U.K., 1993.
(17) Kan, H.; Ferry, J.; Fetters, L. *Macromolecules* **1980**, *13*, 1571.
(18) Klucker, R.; Schosseler, F. *Macromolecules* **1997**, *30*, 4228.
(19) Klucker, R.; Munch, J. P.; Schosseler, F. *Macromolecules* **1997**, *30*, 3839.
(20) de Gennes, P. G. *Scaling Concepts in Polymer Physics*; Cornell University Press: Ithaca, NY, 1979.

MA970158C